Electronic Supporting Information

Direct-Write Liquid Phase Transformations with a Scanning Transmission Electron Microscope

By *Raymond R. Unocic*, Andrew R. Lupini, Albina Y. Borisevich, David A. Cullen, Sergei V. Kalinin, Stephen Jesse**

Electron energy loss spectroscopy (EELS) measurements of fluid layer thickness. A 150 nm spacer microchip was used in these experiments in order to control the fluid layer thickness. The silicon nitride membrane will bow due to the pressure differential that is created between the high vacuum environment of the TEM and the atmospheric pressure within the liquid cell. Previously, it has been shown that electron energy loss spectroscopy can be used to determine the fluid layer thickness from the low loss region of the EEL spectra, which include the zero-loss peak and plasmon peak.[1-3] In the direct-write liquid STEM nanolithography results presented in the manuscript, the experiments were performed in the corner of the silicon nitride membrane close to the silicon support, where membrane bowing is less pronounced. To estimate the fluid layer thickness we use EELS to acquire a spectrum from the corner region of the liquid cell. **Figures S1a-b** are before an after ADF STEM images from where the liquid EELS measurement were acquired. Note that Pd deposition occurs during the EELS measurements as shown in **Figure S1b**. The corresponding low loss EEL spectra is shown in **Figure S1c**. The fluid layer thickness were estimated first by determining the inelastic mean free path (t/λ) which was determined to be 3.31 from **Figure S1c**. The atomic number formula approximation was used to determine λ. An effective atomic number (Z_{eff}) is first determined for scattering through the silicon nitride membranes and water, which is defined as follows:

$$Z_{eff} = \frac{\sum f_n Z_n^{1.3}}{\sum f_n Z_n^{0.3}} \qquad (1)$$

where f_n is the atomic fraction of element (n) and Z_n is the atomic number of element Z_{eff} was determined to be 4.20. λ_i can then be determined through the following approximation:

$$\lambda_i = \frac{106 F E_0}{E_M \ln(2\beta E_0 / E_M)} \qquad (2)$$

where F is the relativistic factor for 300 kV (0.51), E_o is the accelerating voltage (300 kV), β is the collection semi-angle (30 mrad), and E_M is defined as:

$$E_M = 7.6 Z_{eff}^{0.36} \quad (3)$$

From these calculations, λ_i was determined to be 176.7 nm and given that the measured value for t/λ was 3.31, the total thickness (t) was approximately 575 nm. By subtracting out the 100 nm thickness contribution from the silicon nitride membrane, the fluid layer thikcness is then estimated to be 475 nm. These results show that for a 150 nm spacer, the membrane does bow and that the fluid layer thickness increases to approximately 475 nm in the region where the direct-write experiments were performed.

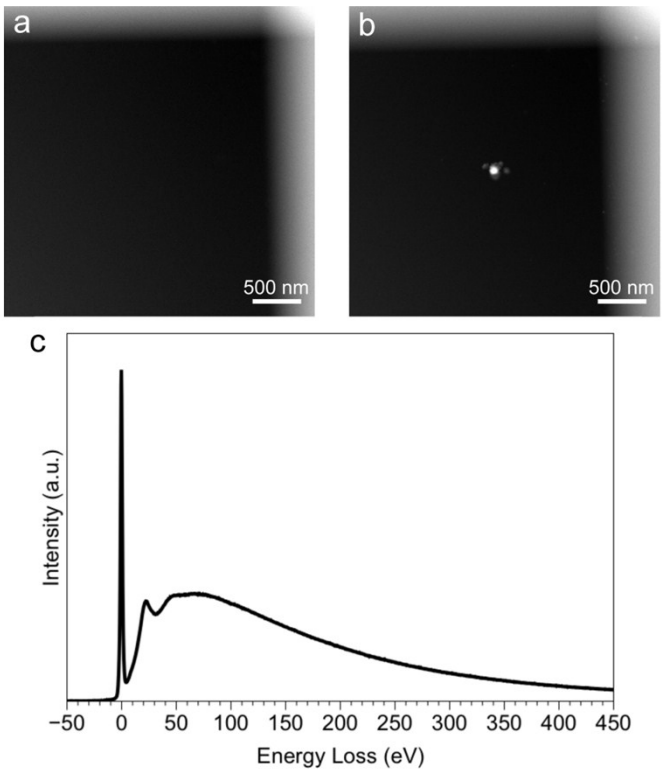

Figure S1. Fluid layer thickness measurement using EELS. (a) ADF STEM image of the liquid cell near the corner where the freestanding silicon nitride membrane meets the silicon support. (b) ADF STEM image where the EELS measurement was acquired as marked by a Pd deposit that formed during electron beam induced deposition. (c) Corresponding low-loss EEL spectra from the measurement in Figure S1b.

Image analysis of Pd deposits. To determine the size of the Pd deposits, quantitative image analysis was performed using Photoshop and Fovea Pro 4.0 software. There were two distinct

features that can be seen in the ADF STEM images following the radiolytic depositon of Pd in the 5 x 5 array patterns presented in **Figure 2** in the main manuscript and **Figures S3-S4** in the supplementary information. A central bright circular region that is uniform in size exists often with irregular shaped features that emanate from the central portion of the deposit. This is more pronounced at higher electron doses. These are most likely Pd nanocrystals that nucleated and grew directly on and from the central deposit. Here, we first analyze the size of the central deposit by line intensity profile measurements and then we analyze the entire feature and report this in terms of the equivalent diameter. **Figure S2a** shows an example of the line intensity profile measurements from **Figure 2d** (points 21-25) in the manuscript. As can be seen, the width of the deposit increases as a function of electron dose. Full width at half-maximum (FWHM) was used to determine the size of the deposit from the line profile. (**Figure S2b**) The line width was increased for better signal-to-noise of the line profile, as illustrated in the yellow-boxed portion in **Figure S1a**.

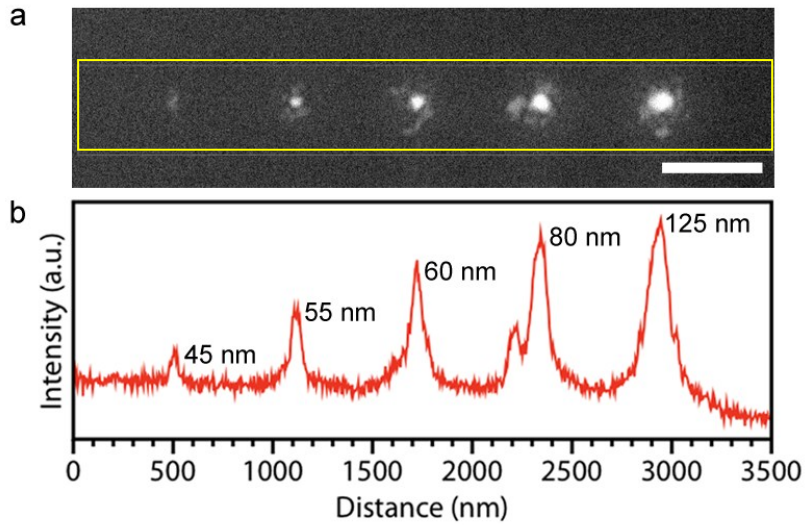

Figure S2. Quantitative image analysis of deposit size. (a) Cropped ADF STEM image from Column 5 (Points 21-25) of Figure 2d with (b) corresponding line intensity profile measurements of deposit size as a function of increasing electron dose. Scale bar is 500 nm.

Influence of electron dose on Pd deposition size scale and morphology.

Bi-level thresholding was first performed on the ADF STEM images then quantitatively analyzed using Fovea Pro image analysis software in Photoshop. The equivalent diameter was measured for the two leftmost columns where the Pd deposits remained intact on the silicon nitride membrane. For each of the doses used in **Figure 5a-c**, there were 10 measurements of equivalent diameter.

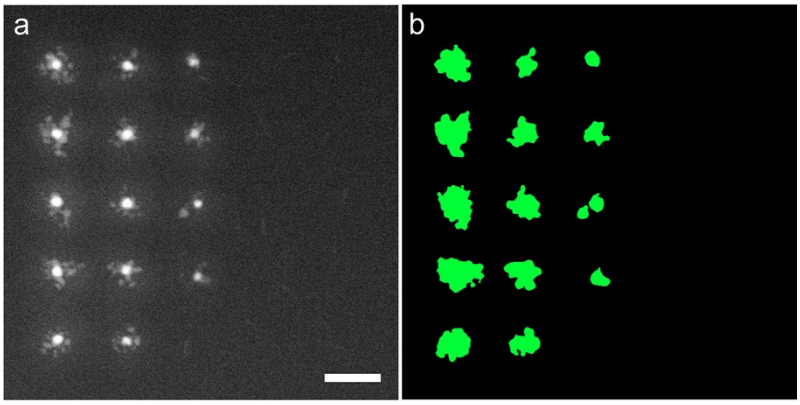

Figure S3. Equivalent diameter measurements of Pd deposit size. (a) ADF STEM image from Figure 5a and (b) bi-level thresholding. Scale bar is 500nm.

***In situ* reaction monitoring.** Here, we demonstrate the ability to monitor the STEM signal intensity during Pd deposition by simultaneously acquiring the BF and ADF STEM signal as a function of time for the 5 x 5 array of deposition points from **Figure 5b** in the main manuscript. In BF STEM (**Figure S4a**), the signal gets darker during Pd deposition when imaged with the BF STEM detector and gets brighter during deposition when imaged with the ADF STEM detector (**Figure S4b**). For each deposit in the 5 x 5 array, the BF and ADF signals were acquired as a function of dwell time, which is shown in **Figure S4c-d**. The asymptotic change in the signal can be readily understood by examining the ADF STEM signal. The intensity of the ADF STEM image is dependent upon atomic number and thickness. Since Pd has a high atomic number (Z-46), as compared to the background, and its deposit gets thicker as a function of time; therefore, the ADF STEM signal will increase. In each of the reaction-monitoring curve, the same trend is recorded even though the post-mortem BF and ADF STEM image shows and absence of a Pd deposit. This provides evidence that Pd was deposited but during the nanofabrication process, some of the deposits have become physically detached from the silicon nitride membrane.

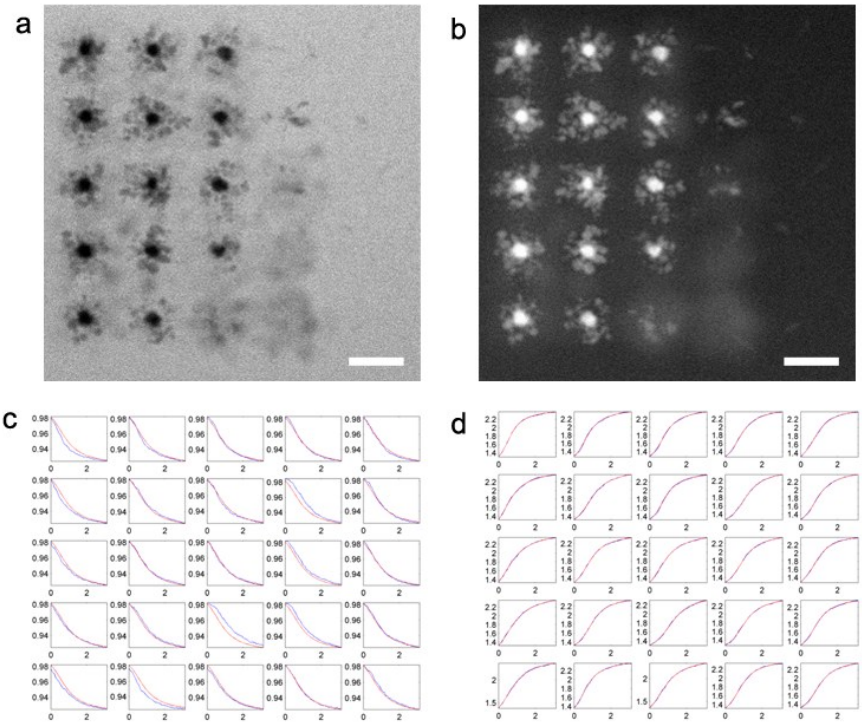

Figure S4. Correlative *in situ* reaction spectroscopy measurements. a) BF and b) ADF STEM images from Figure 5b and corresponding c) BF and d) ADF detector response for each Pd deposit. "Blue" curves are experimental measurements and "red" curves are the experimental fitting results according to Equation 2.

Supporting Information References:

[1] M. E. Holtz, Y. Yu, J. Gao, H. D. Abruña, D. A. Muller, *Microscopy and Microanalysis* **2013**, *19*, 1027.

[2] K. L. Jungjohann, J. E. Evans, J. A. Aguiar, I. Arslan, N. D. Browning, *Microscopy and Microanalysis* **2012**, *18*, 621.

[3] R. R. Unocic, L. Baggetto, G. M. Veith, J. A. Aguiar, K. A. Unocic, R. L. Sacci, N. J. Dudney, K. L. More, *Chemical Communications* **2015**, *51*, 16377.